This is a pre-print of the article:

Bianchi, F. D., R. Mantz, and C. F. Christiansen. "Control Of Variable-Speed Wind Turbines by LPV Gain Scheduling". *Wind Energy*, vol. 7, no. 1, pp. 1–8, 2004.

DOI: 10.1002/we.103

Url: http://onlinelibrary.wiley.com/doi/10.1002/we.103/abstract;jsessionid=487B10FE373210F844273BA69E6C411A.f03t04

Control of variable-speed wind turbines by LPV gain scheduling

F.D.Bianchi * R.J.Mantz † C.F.Christiansen ‡

Wind Energy, John Wiley & Sons, vol. 7, pág. 1-8, 2004.

Abstract

This paper considers gain scheduling control of variable-speed wind energy conversion systems (WECS) in the context of linear parameter varying systems. The typical problems of the classic gain scheduling techniques, such as stability guarantees, undesirable transient responses in the controllers commutations and arduous design procedures, can be avoided with this new formulation. A model of a variable-speed WECS expressed in the LPV form and an optimal LPV gain scheduling control strategy are presented.

Keywords: Linear parameter-varying systems, gain scheduling, wind energy conversion systems, wind turbines.

1 Introduction

Better conversion efficiency and less dynamic loads are two commonly cited advantages of variable-speed wind energy conversion systems (WECS). However, these advantages only become evident with a suitable control strategy [1, 2]. Also, it is known that variable-speed WECS present nonlinear dynamic behavior [3]. Among the control strategies for nonlinear systems, gain scheduling techniques are used in many wind turbine controls [4, 5].

An interesting feature of gain scheduling techniques is their ability to apply powerful linear tools to nonlinear systems. In these approaches, the system is linearized in several operating points, and then a linear controller is designed for each linearized system. In between the selected operating points, the corresponding linear controller is obtained by

*CONICET, Laboratorio de Electrónica Industrial, Control e Instrumentación (LEICI), Facultad de Ingeniería, Universidad Nacional de La Plata, CC 91, 1900 La Plata, Argentina. Phone/Fax: 54-221-4259306. E-mail: fbianchi@ing.unlp.edu.ar. The author to whom correspondence should be addressed

†CICpBA, Laboratorio de Electrónica Industrial, Control e Instrumentación (LEICI), Facultad de Ingeniería, Universidad Nacional de La Plata, CC 91, 1900 La Plata, Argentina.

‡Laboratorio de Electrónica Industrial, Control e Instrumentación (LEICI), Facultad de Ingeniería, Universidad Nacional de La Plata, CC 91, 1900 La Plata, Argentina.

interpolation, resulting in a global control. The linear controller applied at a particular operating point is established by the termed scheduling variables measured in real-time.

In spite of their extended use, classic gain scheduling techniques only assure performance and stability at each operating point where the linear controllers are designed [6]. Besides, the design of the set of linear controllers and later interpolation stage may be a very arduous task. Linear Parameter Varying (LPV) systems proposed by Shamma and Athans [6] can avoid the mentioned difficulties. These systems can be considered as a particular case of Linear Time Varying (LTV) systems where the matrices of the state model are continuous and fixed functions of the scheduling variable or parameter $\theta(t)$ which are assumed in a bounded set Θ [7].

Recent LPV gain scheduling approaches present three interesting features. First, the controller is considered as an entity. That is, only one controller is designed, and the interpolation stage is avoided. Second, the resulting controller guarantees stability and performance even though the scheduling variables are changing quickly. And third, optimal controllers can be obtained solving a convex optimization problem [7, 8] with efficient computer packages [9, 10].

This paper deals with the control of variable-speed WECS in the context of LPV systems. In particular, an optimal LPV gain scheduling strategy, which achieves a compromise between conversion efficiency and dynamic loads, is presented.

2 LPV model for WECS

2.1 System description

The WECS considered in this work consists of a wind turbine, an induction generator, and an electronic converter. This last one controls the generator torque, allowing variable-speed operation. A gearbox adapts the rotational speeds of the wind turbine and the electric generator. The system is connected to a stiff grid that can absorb all the power supplied by the wind turbine without considerable change neither in voltage nor in frequency.

It is considered a wind turbine with only one dominant resonant mode, modelled as a series of inertias linked by flexible shafts with friction [11]. In this case, the dynamic equations for the WECS result

$$J_t\dot{\omega} = Q_a - Q, \tag{1}$$

$$\dot{Q} = K_s(\omega - \omega_g) + B_s(\dot{\omega} - \dot{\omega_g}), \tag{2}$$

$$J_g\dot{\omega}_g = Q - Q_g \tag{3}$$

where J_t and J_g are the moments of inertia of the wind turbine and the generator respectively, K_s is the stiffness coefficient, B_s is the friction coefficient, Q is the shaft torque, ω is the rotational turbine speed, and ω_g is the generator speed (all parameters are assumed on the turbine side).

The aerodynamic torque Q_a has the following expression

$$Q_a = \frac{1}{2}\rho\pi R^3 C_q(\lambda) V^2 \tag{4}$$

where ρ is the air density, R is the turbine radio, V is the wind speed, λ is the tip-speed ratio defined as $R\omega/V$, and $C_q(\lambda)$ is the torque coefficient.

Assuming small slip and constant voltage-frequency relationship, the generator torque Q_g is linear in ω_g

$$Q_g = Q_{g1}\omega_g + Q_{g2}\omega_s \tag{5}$$

where Q_{g1} and Q_{g2} are the linearization constants.

2.2 LPV model

Usually, the torque coefficient is only known in some values of λ. Even so, an expression can be obtained if $C_q(\lambda)$ is approximated in the operating region by a second order polynomial [11]

$$C_q = c_2\lambda^2 + c_1\lambda + c_0. \tag{6}$$

Then, using the previous approximation and linearizing (4) at a generic operating point defined by the mean wind speed v_m and the mean turbine speed ω_m, the aerodynamic torque results

$$Q_a = a(v_m, \omega_m)\ \hat{\omega} + b(v_m, \omega_m)\ \hat{v} \tag{7}$$

where

$$\begin{aligned}
\hat{\omega} &= \omega - \omega_m, \\
\hat{v} &= V - v_m, \\
a(v_m, \omega_m) &= \left.\frac{\partial Q_a}{\partial \omega}\right|_{v_m,\omega_m} = \frac{\pi\rho R^4 c_1}{2}\ v_m + \pi\rho R^5 c_2\ \omega_m, \\
b(v_m, \omega_m) &= \left.\frac{\partial Q_a}{\partial v}\right|_{v_m,\omega_m} = \pi\rho R^3 c_0\ v_m + \frac{\pi\rho R^4 c_1}{2}\ \omega_m.
\end{aligned}$$

Finally, replacing Q_a in (1) with (7), the WECS is expressed in the LPV form

$$\begin{aligned}
\dot{x} &= A(\theta)\ x + B(\theta)\ u, \\
y &= C(\theta)\ x
\end{aligned} \tag{8}$$

where

$$x^T = \left[\begin{array}{ccc} \hat{\omega} & Q & \omega_g \end{array} \right], \qquad u^T = \left[\begin{array}{cc} v & \omega_s \end{array} \right], \qquad \theta^T = \left[\begin{array}{cc} v_m & \omega_m \end{array} \right],$$

$$A = \left[\begin{array}{ccc} a(v_m,\omega_m)/J_t & -1/J_t & 0 \\ (K_s + B_s a(v_m,\omega_m)/J_t) & -B_s(1/J_t + 1/J_g) & (B_s Q_{g1}/J_g - K_s) \\ 0 & 1/J_g & -Q_{g1}/J_g \end{array} \right],$$

$$B = \left[\begin{array}{cc} b(v_m,\omega_m)/J_t & 0 \\ B_s b(v_m,\omega_m)/J_t & (B_s Q_{g2}/J_g) \\ 0 & -Q_{g2}/J_g \end{array} \right], \qquad C = \left[\begin{array}{ccc} 0 & 1 & 0 \\ 0 & 0 & 1 \end{array} \right].$$

In this model, the parameters are the mean wind speed v_m and the mean turbine speed ω_m. Both variables must be measured to update the controller. However, ω_m is not an accessible variable, so the mean generator speed ω_{gm} is used instead. Note that ω_m and ω_{gm} are coincident since they are steady state values. Also, it is important to observe that $A(\cdot)$ and $B(\cdot)$ are affine functions of the parameters v_m and ω_{gm}.

Fig. 1 shows the bounded set Θ (shaded sector) considered in this work to cover all possible values of v_m and ω_{gm}. The set Θ includes three classic operating regions such as: low wind speed where λ is kept at the optimal value to maximize the conversion efficiency, high wind speed where the generated power is kept below its nominal value, and a intermediate region where ω_{mg} is kept constant to avoid large torque and power peaks. The solid line a, in Fig. 1, corresponds to the trajectory of the operating points in the three regions. The same Θ covers other alternative trajectories that join the low and high wind speed regions in a smooth way to reduce, even more, the aforementioned torque and power peaks. These trajectories are indicated with b and c in Fig. 1 [1, 2].

It should be noted that Θ covers not only the mentioned trajectories but also other operating points outside the trajectories. Although this Θ may lead to little conservative controllers, this choice simplifies considerably the design and the resulting controller.

3 Controller design and simulation results

In LPV gain scheduling approach, the design procedure consists in finding a controller $K(\theta(t))$:

$$\begin{aligned} \dot{\mathbf{x}}_k &= \mathbf{A}_k(\theta)\mathbf{x}_k + \mathbf{B}_k(\theta)\omega_s, \\ \omega_g &= \mathbf{C}_k(\theta)\mathbf{x}_k + \mathbf{D}_k(\theta)\omega_s \end{aligned}$$

such that

$$\|\mathbf{z}\|_2 = \int_{-\infty}^{\infty} \mathbf{z}(t)^T \mathbf{z}(t) dt$$

is minimized when $\|\mathbf{w}\|_2 < 1$ where $\mathbf{w}$ is the input and $\mathbf{z}$ is the output of the closed loop system. Usually, each output z_i is weighted with a transfer, named weighting function, that stresses the frequency range where z_i must be minimized. A suitable choice of these weighting function allows a compromise among the objectives expressed by the signals z_i.

In the case of the considered WECS control, two common objectives are:

1. maximize the conversion efficiency and keep the generated power and the turbine speed below safe limits, in agreement with the wind speed. That is, the wind turbine must work in a trajectory such as a, b, or c in Fig. 1. Hence, this objective can be implemented as a speed reference tracking where the reference ω_{ref} is computed according to one of the mentioned trajectories,

2. avoid lightly damped resonant modes in the closed loop system that may be excited by cyclic disturbances or wind turbulence.

Then, the first step in the controller design is to express the previous objectives as signals z_i that must be minimized. The first objective corresponds to minimize the speed error $e = \omega_{ref} - \omega_g$ when the input is ω_{ref}, and the second corresponds to minimize Q when the input is $\hat{v}$. Thus, it is defined

$$\begin{aligned} \mathbf{z} &= \begin{bmatrix} e & Q \end{bmatrix}^T, \\ \mathbf{w} &= \begin{bmatrix} \omega_{ref} & \hat{v} \end{bmatrix}^T. \end{aligned}$$

The feedback diagram with the selected weighting function, named augmented plant, can be establish as it is shown in Fig. 2 where $P(\theta(t))$ is the LPV model of the WECS. The frequency response of the weighting functions $MW_e(s)$[1] and $W_q(s)$ are presented in Fig. 3. The weight $MW_e(s)$ forces steady state error to zero and allows a higher error in high frequency. That is, $MW_e(s)$ aims to achieve a good reference tracking in low frequency. On the other hand, the weighting function $W_q(s)$ stresses the high frequency range to avoid the lightly damping resonant modes.

Once the feedback diagram and the weighting functions are defined, the controller is designed using any of the available computer packages [9, 10]. Because the matrices $A(\cdot)$, $B(\cdot)$, and $C(\cdot)$ are affine functions of θ, and the bounded set Θ is a polygon with

[1]The decomposition in M and W_e is necessary to satisfy controllability and observability conditions [12]

three vertices θ_1, θ_2, and θ_3, the resulting controller consists of three set of matrices $\{A_{ki}, B_{ki}, C_{ki}, D_{ki}\}$ corresponding to each vertex of Θ [7]. Then, the control algorithm can be summarized in the following steps

1. In the instant t, measure the scheduling variables $\theta(t)$, and compute α_i such that

$$\theta(t) = \sum_{i=1}^{3} \alpha_i(t)\theta_i, \quad \text{with} \quad \sum_{i=1}^{3} \alpha_i(t) = 1, \quad \alpha_i \in \mathbb{R}, \quad \alpha_i > 0. \tag{9}$$

2. With the α_i and the $\{A_{ki}, B_{ki}, C_{ki}, D_{ki}\}$, compute the controller matrices from

$$\begin{bmatrix} A_k(\theta(t)) & B_k(\theta(t)) \\ C_k(\theta(t)) & D_k(\theta(t)) \end{bmatrix} = \sum_{i=1}^{3} \alpha_i(t) \begin{bmatrix} A_{ki} & B_{ki} \\ C_{ki} & D_{ki} \end{bmatrix}. \tag{10}$$

3. Finally, in the instant t, (10) corresponds to the differential equation of a LTI system. Therefore, using any methods for linear controller, compute the control signal ω_s.

The performance achieved by the controller can be observed in the following simulations corresponding to the test signals shown in Fig. 4. The selected wind transitions present different rise time to evaluate the system behavior when it is subjected to several change rates of wind speed.

Fig. 5 and 6 present the reference signal ω_{ref} and the speed error e. In Fig. 5 the simulations correspond to the test signals when the reference is computed according to trajectory b in Fig. 1. On the other hand, Fig. 6 shows the response for trajectories a, b, and c when the test signal is 2 in Fig. 4. It can be observed that in all cases the speed error is considerably small. Obviously, the tracking improves when the references become smoother because the large inertias of the system. Note also that the test signals cover the complete wind speed range and that the operating point of the system varies across Θ.

Fig. 7 presents a simulation corresponding to a realer wind profile. The mean wind speed is near 8.8 m/s, and the turbine speed is close to 4 rad/s, which produces cyclic disturbances that excite the resonant modes at 12 rad/s. In Fig. 7 are shown two responses of the closed loop system with controllers designed using different weight at Q. The thick line and the thin line correspond to $W_q(s)$ in Fig. 3 and without constraint in Q, respectively. It is possible to observe the important reduction of the oscillations that can be achieved.

4 Conclusions

In this paper, the control of variable-speed WECS have been considered in the context of LPV systems, a recent reformulation of the classic gain scheduling problem. Owing to the WECS is expressed as an affine LPV model, and all possible values of the scheduling variables are included in a polygon with three vertices, the proposed controller results in a linear combination of three constant controllers. The typical commutation problems of classic gain scheduling approaches are avoided since the controller is continuously adapted to change in the system dynamics with performance and stability guarantees. These facts with the availability of efficient algorithm to design optimal controllers make the LPV control a very promising approach to use with more complicate models and constraints.

Acknowledgments

This work was supported by the Agencia Nacional para la Promoción Científica y Técnica ANPCyT, the Comisión de Investigaciones Científicas de la prov. de Buenos Aires CICpBA, the Consejo Nacional de Investigaciones Científicas y Técnicas CONICET and the Universidad Nacional de La Plata UNLP.

A Appendix

Parameters corresponding to the 400 kW WECS used in the simulations

$N = 3,$

$R = 17.5\ m,$

$J_t = 160\ Tm^2,$

$J_g = 70\ Tm^2,$

$B_s = 50\ Tm^2/s,$

$K_s = 7500\ Tm^2/s^2.$

References

[1] E. Muljadi, K. Pierce, and P. Migliore. A conservative control strategy for variable-speed stall-regulated wind turbine. 19^{th} *ASME Wind Energy Symposium*, 2000.

[2] W.E. Leithead and B. Connor. Control of variable speed wind turbines: design task. *International Journal of Control*, 73(13):1189–1212, 2000.

[3] L.L. Freris. *Wind Energy Conversion Systems*. Prentice-Hall International, 1990.

[4] T. Ekelund. Modelling and linear quadratic optimal control of wind turbines. Technical Report 306, Control Eng. Lab., Chalmers Univ. of Techn., Göteborg. Sweden., 1997.

[5] W.E. Leithead, D.J. Leith, F. Hardan, and H. Markou. Global gain-scheduling control for variable speed wond turbines. In *Proc. European Wind Energy Conference EWEC '99*, 1999.

[6] J.S. Shamma and M. Athans. Guarantees properties of gain scheduled control for linear parameter-varying plants. *Automatica*, 27(3):559–564, 1991.

[7] P. Apkarian, P. Gahinet, and G. Becker. Self-scheduled $\mathcal{H}_\infty$ control of linear parameter-varing systems: A design example. *Automatica*, 31:1251–1261, 1995.

[8] G. Becker and A. Packard. Robust performance of linear parametrically varying systems using parametrically-dependent linear feedback. *Systems and Control Letters*, 23:205–215, 1994.

[9] P. Gahinet, A. Nemirovskii, A.J. Laud, and M. Chilali. *LMI Control Toolbox*. The Mathworks Inc., 1994.

[10] L. El Ghaoui, Nikoukhah R., and F. Delebecque. *LMITOOL: a front-end for LMI optimization, User's guide*, February 1995.

[11] P. Novak. On the modelling and partial-load control of variable-speed wind turbines. Technical Report 206L, Control Eng. Lab., Chalmers Univ. of Techn., Göteborg. Sweden., 1995.

[12] K. Zhou. *Essential of Robust Control*. Prentice Hall, Upper Saddle River, New Jersey, 1998.

Figure Captions

Figure 1. Parameter vector trajectories $\theta(t)$ and bounded set Θ.

Figure 2. Block diagram of the augmented plant.

Figure 3. Weighting functions.

Figure 4. Test wind speed signals used in the simulations.

Figure 5. Reference and speed error corresponding to the four test signal in Fig. 4 and the trajectory b in Fig. 1.

Figure 6. Reference and speed error corresponding to the trajectories a, b, and c in Fig. 1 and the test signal 2 in Fig. 4.

Figure 7. Shaft torque for the closed loop system with controllers designed using $W_q(s)$ in Fig. 3 (thick line) and without constraint at Q (thin line).

Figures

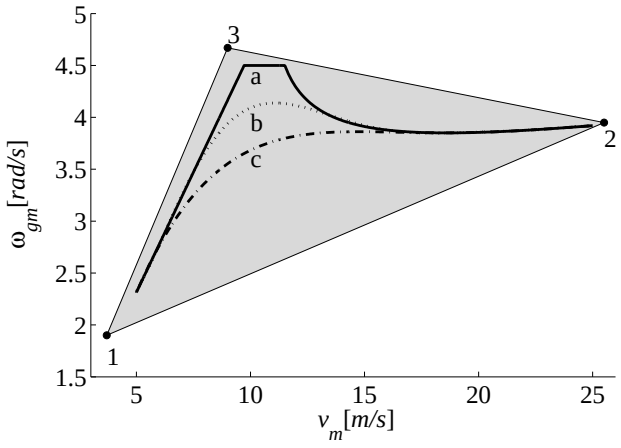

Figure 1: Parameter vector trajectories $\theta(t)$ and bounded set Θ.

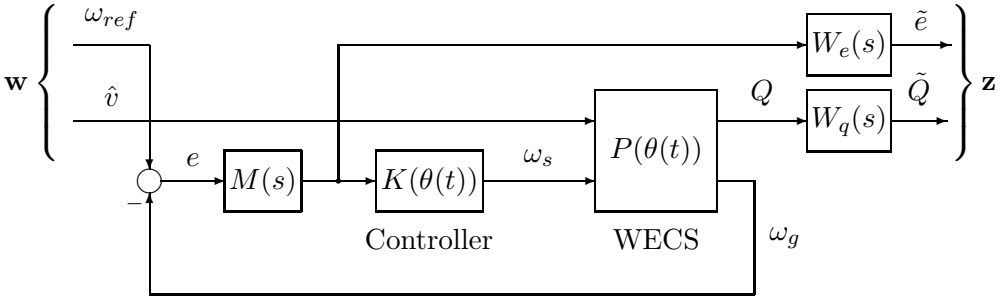

Figure 2: Block diagram of the augmented plant.

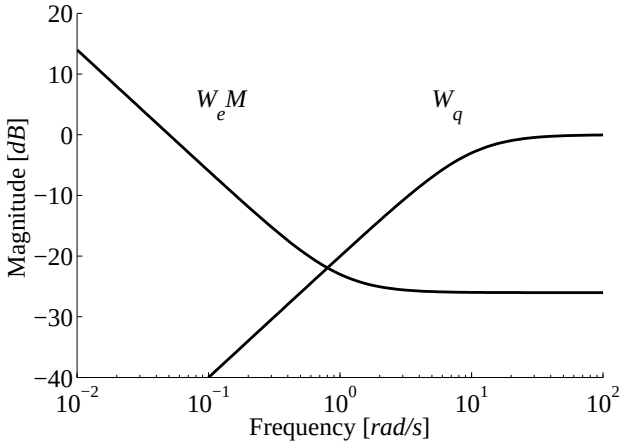

Figure 3: Weighting functions.

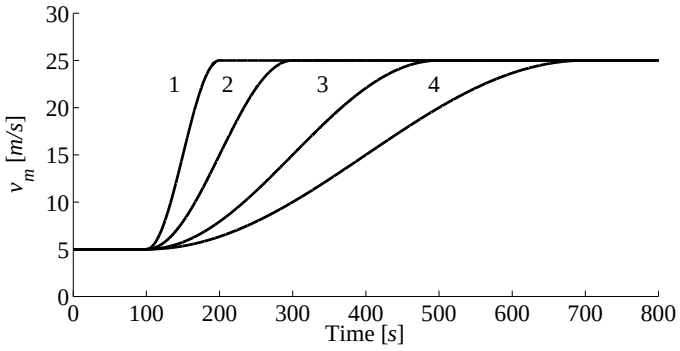

Figure 4: Test wind speed signals used in the simulations.

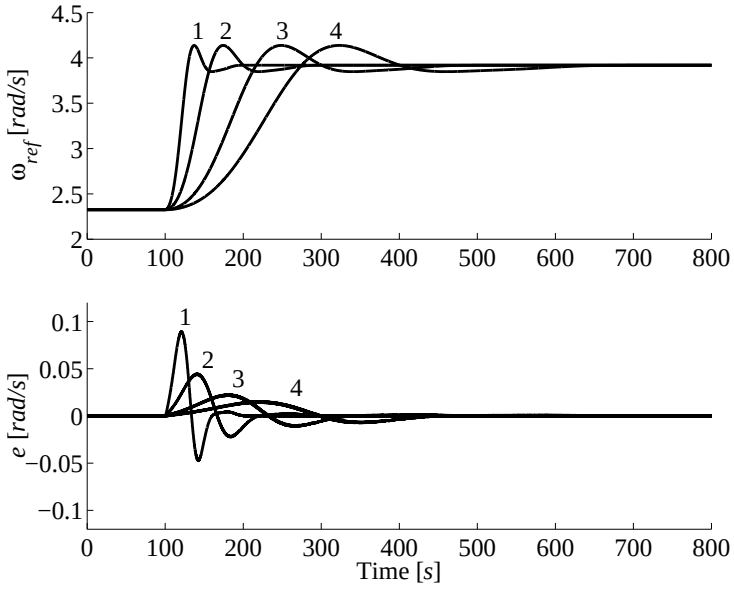

Figure 5: Reference and speed error corresponding to the four test signal in Fig. 4 and the trajectory b in Fig. 1.

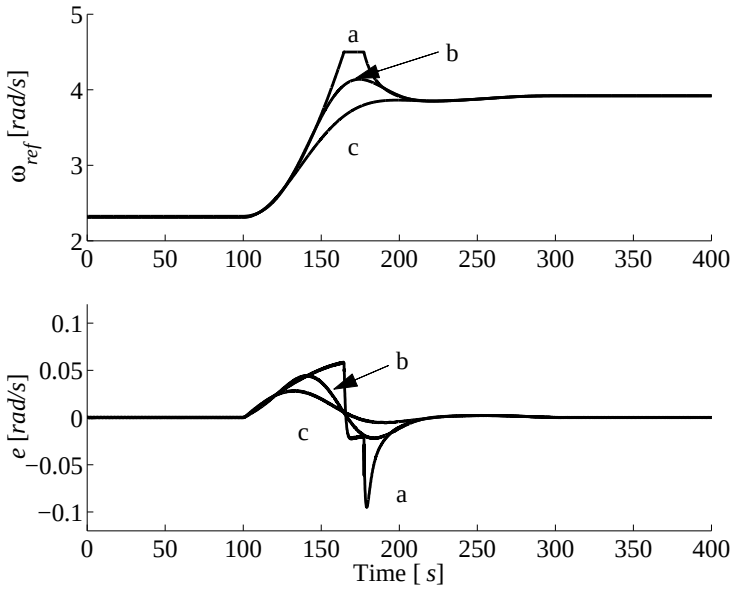

Figure 6: Reference and speed error corresponding to the trajectories a, b, and c in Fig. 1 and the test signal 2 in Fig. 4.

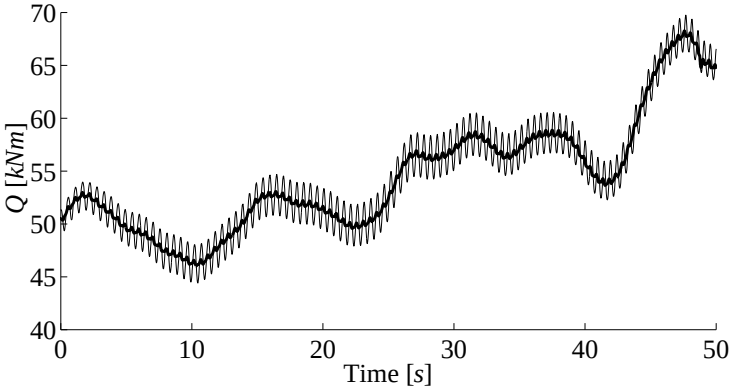

Figure 7: Shaft torque for the closed loop system with controllers designed using $W_q(s)$ in Fig. 3 (thick line) and without constraint at Q (thin line).